Hindawi Publishing Corporation
International Journal of Photoenergy
Volume 2014, Article ID 653206, 6 pages
http://dx.doi.org/10.1155/2014/653206

Research Article

Effect of Multijunction Approach on Electrical Measurements of Silicon and Germanium Alloy Based Thin-Film Solar Cell Using AMPS-1D

Somenath Chatterjee,[1] Sumeet Singh,[1] and Himangshu Pal[2]

[1] *Center for Materials Science & Nanotechnology, Sikkim Manipal Institute of Technology, Majitar, Sikkim 737136, India*
[2] *Applied Electronics and Instrumentation Engineering Department, Sikkim Manipal Institute of Technology, Majitar, Sikkim 737136, India*

Correspondence should be addressed to Somenath Chatterjee; somenath@gmail.com

Received 29 July 2013; Accepted 23 October 2013; Published 29 January 2014

Academic Editor: Francesco Bonaccorso

Multijunction solar cells designed from silicon (Si)-germanium (Ge) alloy based semiconductor materials exhibit high theoretical efficiencies (19.6%) compared to the single junction one. The modeling calculations for all solar cells are done by AMPS 1D simulator. The structure of multi-junction i-layer is designed using heterolayers, starting from pure crystalline Si and increase of Ge mole fraction by 25% until pure Ge layer is reached. The top layer has the largest band gap, while the bottom layer has the smallest bandgap. This design allows less energetic photons to pass through the upper layer(s) and be absorbed by the layer below, which increases the overall efficiency of the solar cell. Material parameters required to model the absorber layers are calculated and incorporated in the AMPS 1D simulator for optimizing of solar cell parameter values. Simulation results show that considerable efficiency enhancement can be obtained from the addition of the multi-junction layer.

1. Introduction

Among all sources of renewable energy, solar energy is attractive due to its abundancy, cleanliness, nontoxicity, and maintenance-free. The thin film technology is considered in second generation of solar cell fabrication due to the reduction of raw materials and cost. Silicon (Si) based thin film solar cell has drawn a lot of attention due to its known processing technology, low process temperature and capability of large-area production [1, 2]. However, improvement in the efficiency of the thin film based solar cells is a challenge for the researchers. Reduction of the excessive energy loss is one of the methods to increase the cell efficiency in thin film based approach. Martins et al. [3] achieved 9.12% efficiency for single junction solar cell using nanostructured hydrogenated silicon material as an intrinsic layer.

More than one absorber layers with different band gaps (i.e., multijunction structures) is applied to effectively convert the photo energy into electricity due to use of additional region from solar spectrum. The efficiency of a single solar cell can be enhanced by a tandem structure consisting of an amorphous and a microcrystalline (mc) layer in stack, with band gaps of about 1.7 and 1.2 eV, respectively. Stabilized efficiency of 11.7% has been reported for a micromorph tandem solar cell (a-Si:H/mc-Si:H) [4]. Also, 12.5% conversion efficiency has been obtained for triple-junction (a-Si:H/nanocrystalline-Si:H/nanocrystalline-Si:H) absorber layer of solar cells [5]. Heterojunction solar cells are formed by a thin a-Si:H layer, sandwiched between n-type nanocrystalline-Si:H and p-type crystalline Si layers, with an efficiency of 14.1% on an area of 2.43 cm^2, as reported elsewhere [6].

A stacked layer structure of Si and germanium (Ge) with different mole fractions can be considered for solar cell, which is affecting the band gaps of the absorber layers and consecutively used the solar spectrum towards the near-infrared region. An a-Si:H/a-SiGe:H/a-SiGe:H triple-junction solar cell with initial efficiencies of 14.6% has been rep-

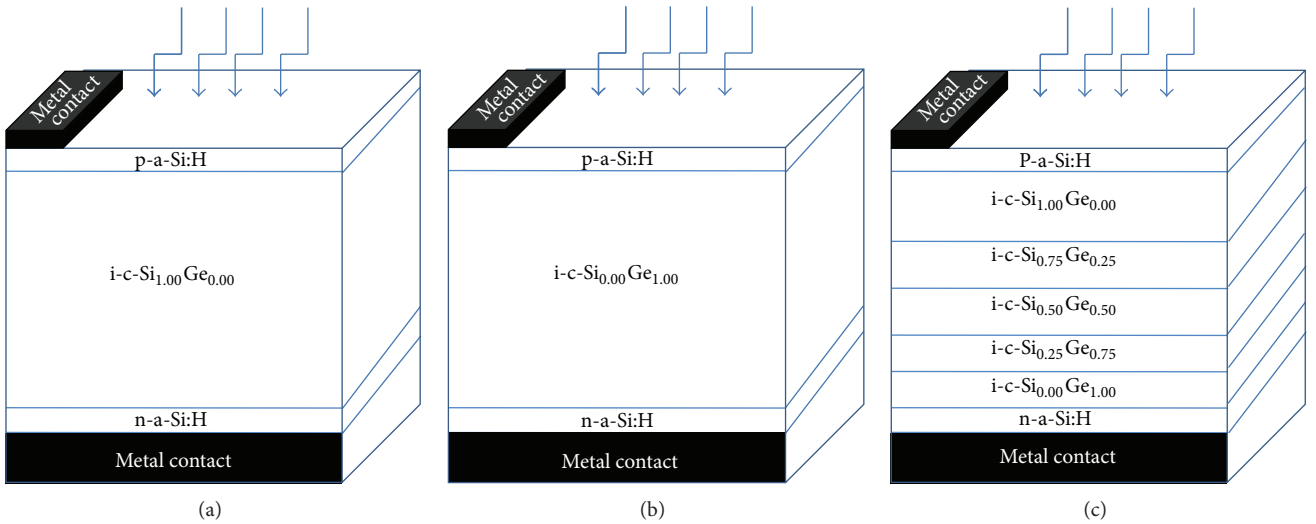

Figure 1: Schematic diagram of solar cell with i-layer crystalline (a) Si, (b) Ge, and (c) $Si_{1-x}Ge_x$ heterolayers.

orted in [7, 8]. However, this value decreases dramatically after light-induced degradation.

AMPS-1D (analysis of microelectronic and photonic structures) is a numerical simulator used for analysing and designing homo- and hetero junctions based semiconductor devices, for example, solar cell [9]. A convenient way to study the role of the various factors, for example, absorption coefficient, mole fraction (x), energy gap, and so forth, on solar parameters (i.e., open circuit voltage (V_{oc}), short circuit current density (J_{sc}), fill factor (FF), and efficiency (η)) of tandem solar cells can be done using AMPS 1D simulator.

In this paper, a combination of crystalline Si and Ge materials as intrinsic layers is employed to design a multistacked heterolayer solar cell using AMPS 1D. A comparative study of the obtained solar parameter values for single junction with stacked hetero-layer (multijunction) is reported here, considering the advantage of band gap tunability and lattice constants with the compositions.

2. Structure of Heterojunction Solar Cells

Enhancement of the device performance in multijunction solar cell compared the single junction one, the materials are selected in such a way to utilize the solar spectrum as well as to avoid the energy loss in a solar cell. Considering the multistacking structure, starting from higher band gap material to lower band gap material, of absorber layer in the design of the solar cell is effective for reduction due to the thermalization losses; that is, gap between the incident photon energy and the optical band gap energy of the photovoltaic material should be minimum.

Figure 1 illustrates the schematic diagram for three solar cell structures to compare the behavior of multistacking with single layer solar cell using AMPS 1D simulator. Figures 1(a) and 1(b) show the basic single-junction structures, where a thin film crystalline Si layer and crystalline Ge layer act as the absorber/intrinsic (i-) layer, respectively, with p- and n-layer consisting of doped p-type and n-type hydrogenated amorphous-Si (a-Si:H) as collector and emitter. In order to achieve high initial efficiencies, one would usually increase the thickness of i-layer. Figure 1(c) shows the multistacking heterostructure of i-layer, starting with pure crystalline Si and increase the Ge mole fraction by 25% until pure Ge layer is reached. Incorporating of Ge into the i-layer, one can reduce the band gap and enhance the long wavelength response. The solar cell structure is completed by aluminum front grid and rear metallization [10].

3. Methods of Simulation

The modeling calculations were executed for the analysis based on Poisson's equation and electron-hole continuity equations using finite differences and the Newton-Raphson technique in AMPS 1D simulator [9] to estimate the steady state band diagram, generation and recombination profile, and carrier transport in different layers of proposed solar cell structures. The input parameter values in layer information part of the AMPS 1D should be provided properly according to the materials used in the different layers of solar cell. The important parameters required to model the i-layer are the band gap (E_g), dielectric constant (ε), intrinsic carrier concentration (n_i), carrier mobilities, effective density of states at valence and conduction band, and the absorption coefficients (α) of absorber materials.

4. Modeling Parameters

4.1. Band/Energy Gap (E_g). The stacked layers are formed by different thicknesses of Si and Ge alloys, which relates to different energy thresholds, absorbing a different band of the solar spectrum over a wide range from 1.12 eV (Si) to 0.66 (Ge) eV, as shown in Figure 1(c). Finding the energy gap values for each layer is essential for AMPS 1D simulator

Table 1: Parameters information for i-layers.

Properties	Material					
	Crystalline Si	Crystalline $Si_{0.75}Ge_{0.25}$	Crystalline $Si_{0.50}Ge_{0.50}$	Crystalline $Si_{0.25}Ge_{0.75}$	Crystalline Ge	Amorphous Si:H [15]
Dielectric constant	11.8	12.93	13.95	14.98	16.0	11.9
Mobility of electron (cm^2/V-s)	1500	2100	2700	3300	3900	20
Mobility of holes (cm^2/V-s)	450	812	1175	1537	1900	2
Energy gap (eV)	1.12	0.96	0.83	0.73	0.66	1.72
Intrinsic carrier concentration n_i (cm^{-3})	1.45×10^{10}	8.3×10^{10}	4.11×10^{11}	1.2×10^{12}	2.4×10^{13}	
Effective density of states in valence band, N_v (cm^{-3})	1.04×10^{19}	9.3×10^{18}	8.2×10^{18}	7.1×10^{18}	6.0×10^{18}	2.5×10^{20}
Effective density of states in conduction band, N_c (cm^{-3})	2.8×10^{19}	7.3×10^{18}	1.46×10^{18}	3.3×10^{17}	1.04×10^{19}	2.5×10^{20}
Electron affinity (eV)	4.05	4.0375	4.025	4.0125	4.0	3.8
Thickness (nm)	2000	1500	900	50	50	

to calculate the absorption coefficients. Crystalline Si and Ge are indirect band gap materials; that is, the valence band maximum and the conduction band minimum are at a different position in k-space [11, 12]. Casado and Ruiz [13] proposed the following energy gap (E_g) equation with Ge mole fraction (x) in $Si_{1-x}Ge_x$ alloy for $x < 0.87$:

$$E_{g_{Si_{1-x}Ge_x}} = (1-x) \cdot E_{g_{Si}} + x \cdot E_{g_{Ge}} - \beta_j \cdot x \cdot (1-x), \quad (1)$$

where $E_{g_{Si}}$ and $E_{g_{Ge}}$ are the energy gap for pure Si and Ge materials, x is the Ge mole fraction, and $\beta_j = 0.25$ eV is the bending factor for indirect band gap materials, respectively. The calculated band gap values are shown in Table 1.

4.2. Density of States. The conductivity (σ) of any semiconductor can be defined as

$$\sigma = q\left(\mu_n n + \mu_p p\right), \quad (2)$$

where n and p are the electron and hole concentration, μ_n and μ_p are the electron and hole mobilities, respectively, and q is the electronic charge. Furthermore, in equilibrium and using the Maxwell-Boltzmann approximation for the carrier concentrations as a function of the Fermi level, the carrier concentrations can be written as [14]

$$n = N_c \exp\left(\frac{E_f - E_c}{kT}\right), \qquad p = N_v \exp\left(\frac{E_v - E_f}{kT}\right), \quad (3)$$

where N_v and N_c are the effective density of states in the valence and conduction band, respectively, E_f is the Fermi level, E_v and E_c are the valence band and the conduction band mobility edges, respectively. k is the Boltzmann constant and T is the temperature, the product of k and T is called the thermal energy and it is 0.026 eV at room temperature.

The parameter values of hydrogenated amorphous silicon (amorphous Si:H) [15] as intrinsic layer are mentioned in Table 1 for showing the comparison with the crystalline Si and crystalline Ge materials. The numerical simulation requires a model for the effective density of states in the layers. For the density of localized states in the mobility gap, it has been assumed that there are both acceptor-like states (in the upper half of the gap) and donor-like states (in the lower half of the gap). Finding the exact values of density of states for different layers is very crucial. The following equations are used to calculate the effective density of states in conduction band ($N_{c_{SiGe}}$) and valance band ($N_{v_{SiGe}}$) for different $Si_{1-x}Ge_x$ heterolayers [14]:

$$N_{v_{SiGe}} = [0.6x + 1.04(1-x)] \cdot 10^{19}/\text{cm}^3, \quad (4)$$

$$n_{i_{SiGe}}^2 = N_{c_{SiGe}} \cdot N_{v_{SiGe}} \cdot \exp\left[-\frac{E_g}{kT}\right], \quad (5)$$

where $n_{i_{SiGe}}$ is the intrinsic carrier concentration, E_g is the energy gap, and x is the Ge mole fraction of $Si_{1-x}Ge_x$ heterolayers. The values of $n_{i_{SiGe}}$ have been calculated from a graphical representation of $n_{i_{SiGe}}$ with Ge content as shown in Koschier et al. [16]. One can easily find the $N_{c_{SiGe}}$ value by estimating the $N_{v_{SiGe}}$ and $n_{i_{SiGe}}$ values in (5) for a particular Ge mole fraction (x). The $n_{i_{SiGe}}$, $N_{v_{SiGe}}$, and $N_{c_{SiGe}}$ values for different x values in $Si_{1-x}Ge_x$ heterolayers are given in Table 1.

4.3. Dielectric Constant (ε). The optical properties of different layers are specified by the relative dielectric constant or permittivity (ε_{SiGe}). The following equation is used to find the ε_{SiGe} for different $Si_{1-x}Ge_x$ layers [17] and the values are given in Table 1:

$$\varepsilon_{SiGe} = 11.8 + 4.2 \cdot x. \quad (6)$$

4.4. Absorption Coefficient. One of the significant factors for the analysis of SiGe based solar cell device is the calculation of absorption coefficient in the alloy layers. Optical absorption in semiconductor is realized through switch of energy from photons to electrons which allows transitions of electrons

from the valence band to the conduction band and therefore the creation of electron-hole pairs. The absorption coefficient (α) due to direct transitions for photons with energy greater than the direct energy gap is given by

$$\alpha = A \cdot \sqrt{h\nu - E_g}, \tag{7}$$

where A is the experimentally derived coefficients, h is Planck's constant, and ν is the frequency of the absorbed photon. However, (7) provides only the vertical transitions in the k-space, but not the change in momentum. Braunstein et al. [18] showed the phonon assisted transitions, two-step transitions, where both energy and momentum are conserved for indirect band gap semiconductor materials (like Si, Ge, or SiGe alloys). The corresponding absorption coefficient values ($\alpha_{\text{absorption SiGe}}$) of SiGe alloys are determined by the following equation, known as the Macfarlane-Roberts expression [19]:

$$\alpha_{\text{absorption, SiGe}} = A \cdot \left[\frac{\left(h\nu - E_g - \overline{E_{\text{ph}}}\right)^2}{1 - \exp\left(-E_{\text{ph}}/kT\right)} + \frac{\left(h\nu - E_g + \overline{E_{\text{ph}}}\right)^2}{\exp\left(-\overline{E_{\text{ph}}}/kT\right) - 1} \right], \tag{8}$$

where $\overline{E_{\text{ph}}}$ is the average energy of all contributed phonon and A is average weighing factor of the absorption coefficients. The above equation expresses two different activities: Phonon assisted absorption (i.e., $E_g - \overline{E_{\text{ph}}}$) and phonon assisted emission process (i.e., $E_g + \overline{E_{\text{ph}}}$).

Polleux and Rumelhard [19] applied (8) for finding the absorption coefficient of SiGe alloy layers. Experimentally obtained $\alpha_{\text{absorption SiGe}}$ values from other works of the literature are fitted well with (8) as shown by Polleux and Rumelhard [19]. Figure 2 shows the absorption coefficient curves with solar spectrum for different mole fractions of Ge in $Si_{1-x}Ge_x$ heterolayers. The curves are obtained using (8) with consideration that A and $\overline{E_{\text{ph}}}$ values are 3200 and 50 meV, respectively applicable for SiGe alloys [20]. According to Figure 2, it is observed that $\alpha_{\text{absorption SiGe}}$ is increased with x in $Si_{1-x}Ge_x$ heterolayers when plotting them against the incident energy. Proper inclusion of these values is important to do the simulation in AMPS 1D.

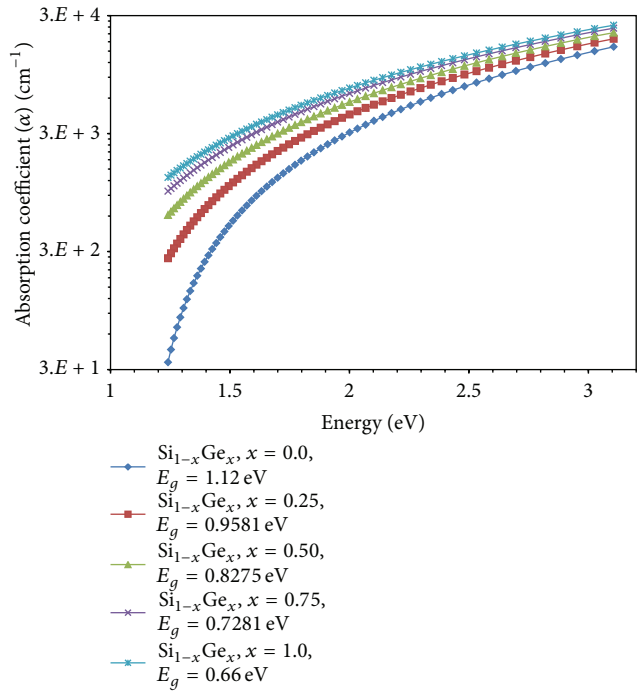

Figure 2: Absorption coefficient with photon energy for pure Si, pure Ge and $Si_{1-x}Ge_x$ heterolayers with different x values used for cell simulation.

Table 2: Different parametric values as used in the simulation for p-layer a-Si:H and n-layer a-Si:H of all three solar cell structures.

Parameters	Layers	
	p-layer a-Si:H	n-layer a-Si:H
Relative permittivity	11.9	11.9
Band gap (eV)	1.82	1.72
Electron mobility (cm^2/V-s)	10	20
Hole mobility (cm^2/V-s)	1	2
Acceptor/donor concentration (cm^{-3})	Acceptor 1×10^{19}	Donor 1×10^{19}
Electron affinity (eV)	3.8	3.8
Thickness (nm)	10	10

5. Results and Discussions of Designed Solar Cell Device

In AMPS 1D simulator, the solar cell device modeling involves the numerical solution of a set of equations, which require the input of device parameters for all the properties (like band gap, electron affinity, doping, mobilities, thicknesses, etc.). General layer parameter values have been incorporated according to different types of layers, which are summarized in Table 1 for intrinsic layer as well as Table 2 for p- and n-layers. In AMPS 1D, one can select the simulation mode either in density of states (DOS) model or lifetime model. The DOS model is considered because of amorphous materials used in p-layer and n-layer (in this study) that have significant defect densities [21].

The operating temperature is set initially at 300 K. The absorption profiles were calculated for the standard global AM1.5 spectrum. A comparison of current density with voltage for crystalline Si, Ge, and $Si_{1-x}Ge_x$ alloy layers is shown in Figure 3. One of the major factors of energy loss in a solar cell is the gap between the incident photon energy and the band gap energy (E_g) of the photovoltaic material. According to Figure 1(c), it is shown that the E_g is varying in the i-layer from 1.12 eV to 0.66 eV for $Si_{1-x}Ge_x$ alloy layer structure, which enhanced the photon absorption probability in the i-layer. In Table 3, the solar cell parametric results are given as obtained from AMPS 1D.

Increasing the number of layers clearly increases the complexity of the whole cell structure. For comparison, the thicknesses of all types of Si and Ge based solar cells

Table 3: Comparison of solar cell parameters for different i-layers.

i-layer	Properties			
	Open circuit voltage, V_{oc} (V)	Short circuit current, J_{sc} (mA/cm^2)	Field factor, FF (%)	Efficiency, η (%)
Crystalline Si	0.991	20.173	0.831	16.601
Crystalline Ge	0.679	31.586	0.333	7.141
Graded crystalline $Si_{1-X}Ge_X$ alloy (x = 0 to 1, with increment 0.25)	0.938	28.202	0.741	19.597

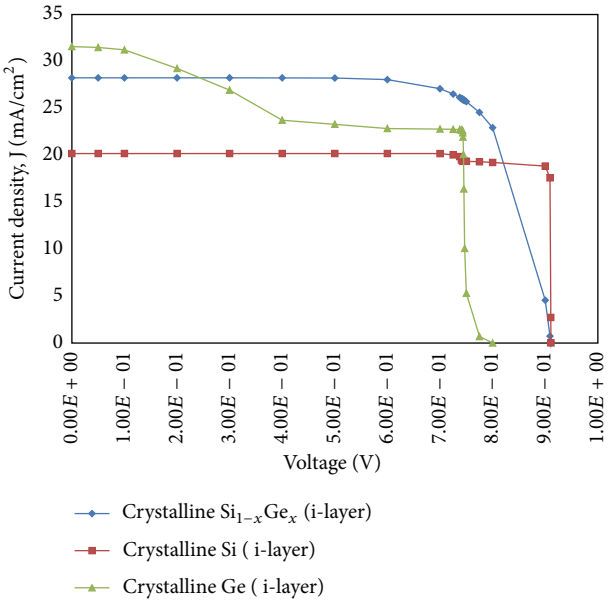

Figure 3: Comparison of current density versus voltage curves for Si, Ge, and $Si_{1-x}Ge_x$ alloy for i-layer in thin-film solar cell structure.

(discussed here) are considered with the same thickness (i.e., 4.52 μm).

According to Table 3, the observed efficiency value is highest for the $Si_{1-x}Ge_x$ alloy based solar cell structure. To optimize the solar cell parameter values for $Si_{1-x}Ge_x$ alloy layers (i-layer), one can precede with the following considerations during simulations in AMPS 1D: (i) thickness of the layers, (ii) top layers with higher energy gap values, (iii) Ge mole fraction (x) variation in crystalline Si for different heterolayers and (iv) providing the proper parametric values (as obtained from Tables 1 and 2) in layer information part of AMPS 1D simulator.

The V_{oc} values for crystalline Si and graded layer structure are around 0.9 V, which is showing no significant change, whereas the J_{sc} is higher in graded layer structure than that of crystalline Si, implying that the carrier collection probability and/or carrier mobility are increased due to the broadening of the spectral response in the i-layer.

Adding Ge to the bottom cell, one can reduce the band gap and enhance the long wavelength response. The top cell is significantly thick compared to the other layers in $Si_{1-x}Ge_x$ heterolayers (as mentioned in Table 2) to produce a current large enough to match the current from the low band gap bottom cell [22]. Another notable observation is that the crystalline Ge based i-layer solar cell shows the highest J_{sc} values, which is common for low band gap material. However, the other solar cell parameter values for crystalline Ge single junction (i.e., V_{oc}, FF, and η) are not promising for solar cell applications (as shown in Table 3).

6. Conclusion

A comparison of the simulated theoretical efficiencies from multijunction and single junction solar cell is discussed here. In order to evaluate the electrical performances of Si and Ge based single and multijunction solar cells, a simulation study is executed using AMPS 1D simulator. Simulation results show that considerable efficiency enhancement can be obtained due to the addition of different bandgap alloy layers in decreasing manner.

Conflict of Interests

The authors declare that there is no conflict of interests regarding the publication of this paper.

Acknowledgment

The authors acknowledge the use of AMPS-1D program developed by Dr. Fonash's group of Pennsylvania State University.

References

[1] S. Benagli, D. Borello, E. Vallat-Sauvain, J. Meier, U. Kroll, and J. Hotzel, "High-efficiency amorphous silicon devices on LPCVD-ZnO TCO prepared in industrial KAI-M R&D reactor," in *Proceedings of the 24th European Photovoltaic Solar Energy Conference*, Hamburg, Germany, 2009.

[2] Ö. Tüzün, Y. Qiu, A. Slaoui et al., "Properties of n-type polycrystalline silicon solar cells formed by aluminium induced crystallization and CVD thickening," *Solar Energy Materials and Solar Cells*, vol. 94, no. 11, pp. 1869–1874, 2010.

[3] R. Martins, L. Raniero, L. Pereira et al., "Nanostructured silicon and its application to solar cells, position sensors and thin film transistors," *Philosophical Magazine*, vol. 89, no. 28–30, pp. 2699–2721, 2009.

[4] M. Yoshimi, T. Sasaki, T. Sawada et al., "High efficiency thin film silicon hybrid solar cell module on 1m2-class large area substrate," in *Proceddings of the 3rd World Conference on Photovoltaic Energy Conversion*, pp. 1566–1569, May 2003.

[5] B. Yan, G. Yue, and S. Guha, "Status of nc-Si:H solar cells at United Solar and roadmap for manufacturing a-Si:H and nc-Si:H based solar panels in amorphous and polycrystalline thin-film silicon science and technology 2007," in *Materials Research Society Symposium Proceeding*, V. Chu, K. Miyazaki, A. Nathan, J. Yang, and H.-W. Zan, Eds., vol. 989, 2007.

[6] Y. Xu, Z. Hu, H. Diao et al., "Heterojunction solar cells with n-type nanocrystalline silicon emitters on p-type c-Si wafers," *Journal of Non-Crystalline Solids*, vol. 352, no. 9–20, pp. 1972–1975, 2006.

[7] J. Yang, B. Yan, and S. Guha, "Amorphous and nanocrystalline silicon-based multi-junction solar cells," *Thin Solid Films*, vol. 487, no. 1-2, pp. 162–169, 2005.

[8] T. Matsui, H. Jia, and M. Kondo, "Thin film solar cells incorporating microcrystalline $Si_{1-x}Ge_x$ as efficient infrared absorber: an application to double junction tandem solar cells," *Progress in Photovoltaics: Research and Applications*, vol. 18, no. 1, pp. 48–53, 2010.

[9] S. Fonash, J. Arch, J. Cuiffi et al., "A Manual for AMPS-1D for Windows 95/ NT a One-Dimensional Device Simulation Program for the Analysis of Microelectronic and Photonic Structures," The Pennsylvania State University, 1997.

[10] N. Jensen, R. M. Hausner, R. B. Bergmann, J. H. Werner, and U. Rau, "Optimization and characterization of amorphous/crystalline silicon heterojunction solar cells," *Progress in Photovoltaics: Research and Applications*, vol. 10, no. 1, pp. 1–13, 2002.

[11] S. Chatterjee and L. K. Bera, "Determination of band discontinuities in silicon heterostructures," *IETE Journal of Research*, vol. 53, no. 3, pp. 199–214, 2007.

[12] D. V. Lang, R. People, J. C. Bean, and A. M. Sergent, "Measurement of the band gap of Ge_xSi_{1-x}/Si strained-layer heterostructures," *Applied Physics Letters*, vol. 47, no. 12, pp. 1333–1335, 1985.

[13] J. Casado and M. Ruiz, "Calculation of properties derived from near-edge band structure in $Si_{1-X}Ge_X$ alloy system," in *Proceedings of the 13th European Photovoltaic Solar Energy Conference and Exhibition (PVSEC '95)*, pp. 1311–1314, Niza , France, 1995.

[14] J. Nelson, *The Physics of Solar Cells*, chapter 2, Imperial College Press, London, UK, 2008.

[15] N. Hernández-Como and A. Morales-Acevedo, "Simulation of hetero-junction silicon solar cells with AMPS-1D," *Solar Energy Materials and Solar Cells*, vol. 94, no. 1, pp. 62–67, 2010.

[16] L. M. Koschier, S. R. Wenham, and M. A. Green, "Modeling and optimization of thin-film devices with $Si_{1-x}Ge_x$ alloys," *IEEE Transactions on Electron Devices*, vol. 46, no. 10, pp. 2111–2115, 1999.

[17] V. Venkataraman, S. Nawal, and M. J. Kumar, "Compact analytical threshold-voltage model of nanoscale fully depleted etrained-silicon on silicon-germanium-on-insulator (SGOI) MOSFETs," *IEEE Transactions on Electron Devices*, vol. 54, no. 3, pp. 554–562, 2007.

[18] R. Braunstein, A. R. Moore, and F. Herman, "Intrinsic optical absorption in germanium-silicon alloys," *Physical Review*, vol. 109, no. 3, pp. 695–710, 1958.

[19] J. L. Polleux and C. Rumelhard, "Optical absorption coefficient determination and physical modelling of strained SiGe/Si photodetectors," in *Proceedings of the 8th IEEE International Symposium on High Performance Electron Devices for Microwave and Optoelectronic Applications (EDMO '00)*, pp. 167–172, November 2000.

[20] A. Vonsovici, L. Vescan, R. Apetz, A. Koster, and K. Schmidt, "Room temperature photocurrent spectroscopy of SiGe/Si p-i-n photodiodes grown by selective epitaxy," *IEEE Transactions on Electron Devices*, vol. 45, no. 2, pp. 538–542, 1998.

[21] R. H. Bube, *Photovoltaic Materials*, Imperial College Press, London, UK, 1998.

[22] J. Yang, A. Banerjee, and S. Guha, "Amorphous silicon based photovoltaics—from earth to the 'final frontier'," *Solar Energy Materials and Solar Cells*, vol. 78, no. 1–4, pp. 597–612, 2003.